ELSEVIER

Journal of Chromatography B, 779 (2002) 283–295

JOURNAL OF CHROMATOGRAPHY B

www.elsevier.com/locate/chromb

Determination of the enantiomerization energy barrier of some 3-hydroxy-1,4-benzodiazepine drugs by supercritical fluid chromatography

Peter Oswald[a], Koen Desmet[b], Pat Sandra[b], Jan Krupčík[a,*], Pavol Májek[a], Daniel W. Armstrong[c]

[a]*Department of Analytical Chemistry, Slovak University of Technology, Radlinského 9, Bratislava 81237, Slovakia*
[b]*Department of Organic Chemistry, University of Ghent, Krijgslaan 281 S4, B-9000 Ghent, Belgium*
[c]*Department of Chemistry, Gilman Hall, Iowa State University, Ames, IA 50011-3111, USA*

Received 22 March 2002; received in revised form 28 May 2002; accepted 30 May 2002

Abstract

The first-order kinetic equation for irreversible reactions was used to determine the enantiomerization barrier of some of 3-hydroxy-1,4-benzodiazepine enantiomers by supercritical fluid chromatography (SFC). The racemates of lorazepam, oxazepam and temazepam were separated by SFC on chiral (*R*,*R*)-Whelk-O1 column with supercritical carbon dioxide containing 12.5% methanol and 0.5% diethylamine as a mobile phase. Peak areas of enantiomers prior to (A_{A0}, A_{B0}) and after the separation (A_A, A_B), used for calculation of the enantiomerization barrier, were determined by computer-assisted peak deconvolution of peak clusters from the chromatograms. It was demonstrated for the first time that using a model for a four-peak cluster produces height precise results, and most closely approximates the published results. The kinetic equation for irreversible reactions was used to determine apparent enantiomerization rate constants. The dependence of the apparent enatiomerization barrier ($\Delta G^{app}_{A\rightarrow B}$, $\Delta G^{app}_{B\rightarrow A}$) on temperature was used to determine apparent activation enthalpy ($\Delta H^{app}_{R\rightarrow S}$, $\Delta H^{app}_{S\rightarrow R}$) and entropy ($\Delta S^{app}_{R\rightarrow S}$, $\Delta S^{app}_{S\rightarrow R}$) for all studied benzodiazepines.

Keywords: Enantiomerization energy barrier; Enantiomer separation; Lorazepam; Temazepam; Oxazepam

1. Introduction

Since 1992, regulatory agencies have required extensive stereochemical information on chiral drugs [1]. Since their discovery in 1957 [2], benzodiazepines have become the most widely prescribed drugs for the treatment of anxiety, insomnia, convulsion and related disorders. The therapeutic efficacy of these compounds has, however, been shown to be enantio-specific [3,4]. Pharmacological studies such as chiral form-stability, interconversion, pharmacokinetic properties and dosage equivalence of chiral therapeutics are required. The enantiomeric separation of these compounds is mostly carried out by chiral gas chromatography (GC) [5], high-performance liquid chromatography (HPLC) [5–16],supercritical fluid chromatography (SFC) [17], micellar capillary electrophoresis (MCE) [18,19] and

*Corresponding author. Tel.: +421-2-5932-5314; fax: +421-2-5292-6043.
E-mail address: krupcik@cvt.stuba.sk (J. Krupčík).

1570-0232/02/$ – see front matter
PII: S1570-0232(02)00396-3

electrochromatography [20,21]. Enantiomers of some 3-hydroxy-1,4-benzodiazepines, however, undergo inversion of their respective configurations at elevated temperatures [8,9,13]. This interconversion, labelled as enantiomerization, is an undesired attribute of some chiral drugs. The extent of interconversion of enantiomers depends on the energy barriers to enantiomerization and can be determined by several methods. Chromatographic techniques are among the most effective methods since enantiomers are separated and analysed on-line, thus requiring only minute amounts of the racemic mixtures, enriched mixture or pure enantiomers [22–32]. During enantioselective chromatography interconversion of the enantiomers may produce a peak cluster composed of a peak of racemized material (plateau) between the two peaks of the enantiomers [23]. The shape of the peak cluster on the chromatogram obtained by separating a racemate is dependent on the interconversion rate of the enantiomers. Dynamic high-performance liquid (DHPLC) chromatography as well as capillary electrophoresis and electrochromatography (DCEC) have been used to study interconversion, for some 3-hydroxy-1,4-benzodiazepines [9,13,15,19,32]. Interconversion of 3-hydroxy-1,4-benzodiazepines occurs due to keto-enol tautomerization [33]. This reaction strongly depends both on temperature as well as stationary and mobile phase composition [8]. When the amount of protic modifier in the mobile phase is decreased, interconversion is reduced. By gradually increasing the amount of acetonitrile in a protic modifier such as ethanol, racemization can be suppressed [34]. This, however, shows that the interconversion barrier depends on the stationary or mobile phase constituents, which influences the rate of interconversion [8].

In our recent study we demonstrated the first use of dynamic supercritical fluid chromatography (DSFC) for the determination of the enatiomerization barrier of *N*-(*p*-methoxybenzyl)-1,3,2-benzodithiazol-1-oxide [35]. The racemate of *N*-(*p*-methoxybenzyl)-1,3,2-benzodithiazol-1-oxide was separated by SFC on chiral (*R,R*)-Whelk-O1 column with supercritical carbon dioxide containing 20% of methanol as a mobile phase. It has been shown that the interconversion of enantiomers in a chromatographic column during the separation process can be described by the first-order kinetic equation for irreversible reactions. Equations derived using the irreversible concept for the calculation of rate constants and energy barriers to enantiomerization also gives results for a high degree of enantiomerization where the reversible approach failed [36].

In the present study, DSFC is applied to determine the enantiomerization barrier of the 3-chiral-1,4-benzodiazepine drugs: lorazepam, temazepam, and oxazepam. The enantiomerization barriers were calculated from the peak areas of enantiomers (A, B) prior to separation (A_{A0}, A_{B0}) and after the separation (A_A, A_B) using the equation derived for the irreversible model. The corresponding peak areas are determined by the computer-assisted deconvolution of the peak cluster obtained after separating the racemate by DSFC. In this method, deconvolution software is used in a new approach where the treated cluster involves four peaks.

2. Theoretical

The direct chromatographic separation of a racemic or enriched mixture of thermolabile enantiomers is known as dynamic enantioselective chromatography [23]. The interconversion of enantiomers (A and B) can be described by a scheme:

$$A \underset{k_{-1}}{\overset{k_1}{\rightleftarrows}} B$$

where k_1 and k_{-1} are the rate constants of the $A \rightarrow B$ and $B \rightarrow A$ interconversion, respectively. In this scheme A denotes the first and B the second eluted enantiomer. Interconversion in stationary systems is considered as a reversible reaction and can be described by the first-order kinetic equation.

Chromatography and electromigration methods, however, are dynamic systems. If the original and the interconverted enantiomers are separated, then conversion in these systems looks irreversible [36] and the $A \rightarrow B$ and $B \rightarrow A$ interconversions can be described by first-order kinetic equation [37] for irreversible concepts.

Apparent rate constants ($k_1^{\mathrm{app}}$and k_{-1}^{app}) which are weighted means of the different interconversion rates in the mobile and the stationary phase [18,32] are used to describe the rate in dynamic chromatography if $A \rightarrow B$ and $B \rightarrow A$ is the reversible or irreversible

interconversion. As routine chromatographic detectors gives equal response for both enantiomers, the apparent rate constants are determined directly from peak areas A_0 and A. The apparent rate constants are calculated for reversible concept from the following equations [18,32]:

$$k_1^{\text{app}} = \frac{1}{2t_{\text{R},A}} \ln \frac{c_{A0}}{2c_A - c_{A0}} = \frac{1}{2t_{\text{R},A}} \ln \frac{A_{A0}}{2A_A - A_{A0}} \quad (1a)$$

or

$$k_{-1}^{\text{app}} = \frac{1}{2t_{\text{R},B}} \ln \frac{c_{B0}}{2c_B - c_{B0}} = \frac{1}{2t_{\text{R}}} \ln \frac{A_{B0}}{2A_B - 2A_{B0}} \quad (1b)$$

For irreversible concept from the equations [36,37]:

$$k_1^{\text{app}} = \frac{1}{t_{\text{R},A}} \ln \frac{c_{A0}}{c_A} = \frac{1}{t_{\text{R},A}} \ln \frac{A_{A0}}{A_A} \quad (2a)$$

or

$$k_1^{\text{app}} = \frac{1}{t_{\text{R},A}} \ln \frac{c_{B0}}{c_B} = \frac{1}{t_{\text{R},B}} \ln \frac{A_{B0}}{A_B} \quad (2b)$$

where t_{R} is the retention time, A is the peak area of the enantiomer A and B at the time prior to separation (at the time $t=0$ peak areas are A_{A0} or A_{B0}) and after the separation (at the time t peak areas are A_A or A_B), respectively.

In dynamic chromatographic and electromigration systems it can be assumed that:

(i) enantiomers (A and B) and products of enantiomerization (enantiomers A' and B' that formed during enantiomerization in the chromatographic column) do not interfere with one another during their migration through the column,

(ii) any brief contacts between enantiomers (A, B and A', B') at a microscopic level do not significantly influence the results.

That is why the interconversion of $A \rightarrow B$ and $B \rightarrow A$ in a racemic mixture can be studied by chromatographic and electromigration methods independently even using racemates as irreversible types of interconversions.

The energy barriers to $A \rightarrow B$ and $B \rightarrow A$ enantiomerization can be found from the apparent rate constants using the Eyring equation [37]:

$$-\Delta G_{A\rightarrow B}^{\text{app}} = RT \ln\left(\frac{hk_1^{\text{app}}}{\kappa k_b T}\right) \quad (3a)$$

or

$$-\Delta G_{B\rightarrow A}^{\text{app}} = RT \ln\left(\frac{hk_{-1}^{\text{app}}}{\kappa k_b T}\right) \quad (3b)$$

where R is the universal gas constant, T is the temperature in K, κ is transmission coefficient, k_{B} is the Boltzmann constant and h is Planck's constant.

The dependence of the apparent enantiomerization barrier ($\Delta G_{A\rightarrow B}^{\text{app}}$, $\Delta G_{B\rightarrow A}^{\text{app}}$) on temperature can be used for the calculation of the apparent activation enthalpy ($\Delta H_{A\rightarrow B}^{\text{app}}$, $\Delta H_{B\rightarrow A}^{\text{app}}$) and entropy ($\Delta S_{A\rightarrow B}^{\text{app}}$, $\Delta S_{B\rightarrow A}^{\text{app}}$) [18,34] using Gibbs–Helmholz equation:

$$\Delta G_{A\rightarrow B}^{\text{app}} = \Delta H_{A\rightarrow B}^{\text{app}} - T\,\Delta S_{A\rightarrow B}^{\text{app}} \quad (4a)$$

or

$$\Delta G_{B\rightarrow A}^{\text{app}} = \Delta H_{B\rightarrow A}^{\text{app}} - T\,\Delta S_{B\rightarrow A}^{\text{app}} \quad (4b)$$

From the above written equations it follows that the enantioselectivity of a chiral selector is responsible for differences in thermodynamic data for both enantiomers. Difference in activation energy is proportional to the enantioselectivity (α) as it follows from following equation:

$$\Delta(\Delta G^{\text{app}}) = \Delta G_{B\rightarrow A}^{\text{app}} - \Delta G_{A\rightarrow B}^{\text{app}} = -RT \ln \frac{t'_{\text{R},B}}{t'_{\text{R},A}} = RT \ln \alpha \quad (5)$$

Fig. 1 shows a free energy interconversion coordinate diagram for the enantioselective interconversion of enantiomer $A \rightarrow B$ and $B \rightarrow A$. From Eq. (5) and Fig. 1 it follows that the more enantioselective a separation system is, the higher the enantiomerization barrier of the compound represented by the second eluted peak shall be. This is why the data calculated for the first eluted peak are less affected by the experimental conditions and to a first approxi-

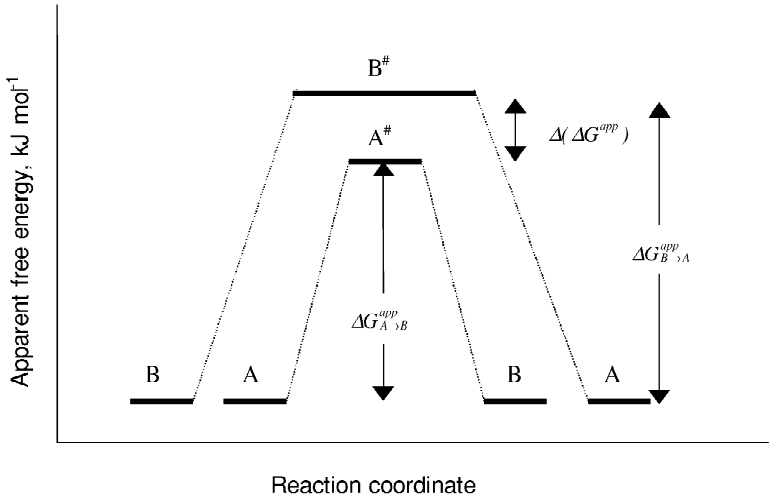

Fig. 1. Free energy interconversion coordinate diagram for the conversion of enantiomer $A \rightarrow B$ and $B \rightarrow A$.

mation they can be tabulated and compared with those data found by classical methods.

Moreover, from the above equations, it follows that the energy barrier to enantiomerization ($\Delta G^{\text{app}}_{A\rightarrow B}$, $\Delta G^{\text{app}}_{B\rightarrow A}$) can be found using dynamic chromatography (DSFC) if the following parameters are known: the temperature (T), the enantiomerization time (t) and the peak areas of the enantiomers prior (A_{A0} or A_{B0}) and after (A_A or B_B) the separation. The temperature is accessible from the experiment. The enantiomerization time and peak areas can be obtained from corresponding chromatograms. Chromatograms obtained by the dynamic chromatographic separation of thermolabile enantiomers consists of a peak cluster in which the overlapped peaks can be resolved by:

(a) multidimensional systems combining two or more single separation systems,

(b) computerized simulation and stochastic methods,

(c) combination of two or more detection systems, from which at least one should be chirospecific, and/or

(d) computer-assisted mathematical deconvolution of overlapped peaks. The number of peaks and a peak shape design belong to basic input parameters in this procedure. This, however, is a particular problem for the systems where the number of peaks in the peak cluster is not known [38,39].

3. Experimental

3.1. Instruments

All the experiments were performed on a HP G1205A SFC (Hewlett-Packard, Little Falls Site, DE, USA), equipped with dual pumps and coupled to a HP 1050 Diode array detector. Data were processed on a HP Windows Chemstation. Two ml min^{-1} of supercritical carbon dioxide containing 20% of methanol at a pressure of 200 bar were used for the separation of *N*-(*p*-methoxybenzyl)-1,3,2-benzodithiazol-1-oxide enantiomers. For the separation of lorazepam, temazepam and oxazepam enantiomers the flow-rates of 1.2–2.4 ml min of supercritical carbon dioxide containing 12.5% methanol with 0.5% diethylamine as modifier were used. Methanol solutions containing 5 mg ml^{-1} of individual analytes were injected using a six-port valve (Valco) equipped with a 10 μl sample loop. For the deconvolution of the chromatograms the Origin software [40] was used. An exponentially modified Gauss function (EMGF) was used as a fitting function [41]. All the calculations were performed on IBM compatible PC computer.

3.2. Column and chemicals

The column used was a (R,R)-Whelk-O1 (25×

0.46 cm I.D., 5 μm) manufactured by Regis (Morton Grove, IL, USA).

SFC-grade carbon dioxide was purchased from Air Liquid (Belgium). HPLC-grade methanol was purchased from Riedel de Haen (Seelze, Germany).

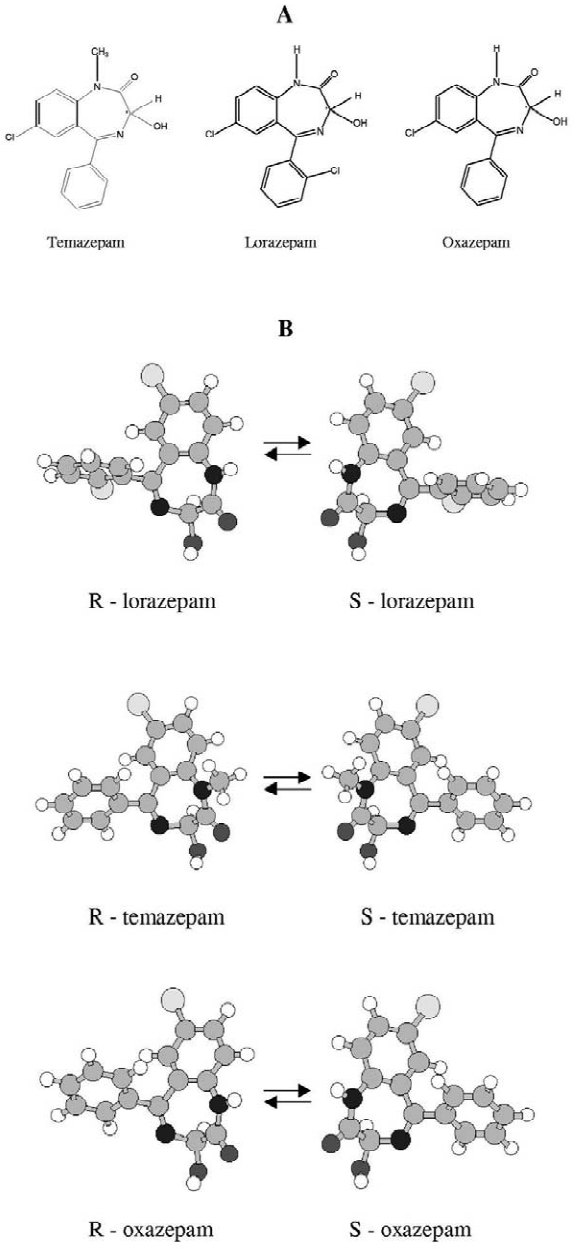

Fig. 2. Schematic of the structures (A) and optimum conformations (B) of the 3-hydroxy-1,4-benzodiazepines evaluated in this study.

Diethylamine (Janssen Chimica, Belgium) was used as an additive in the benzodiazepine analyses.

Lorazepam, oxazepam and temazepam (Fig. 2) were extracted from drugs distributed by Temesta (Wyeth), Seresta (Wyeth) and Levanxol (Pharmacia & Upjohn), respectively. Methanol solutions with the concentration of 5 mg ml^{-1} were prepared for each analyte.

3.3. Theoretical calculations

Optimum conformations corresponding to the energy minima in the gas phase at 0 K of benzodiazepines, shown in Fig. 1B, were calculated on the semiempirical level using the AM1 method [42], which is implemented in the HyperChem for Windows [43]. The starting geometries of considered molecules were created by the molecular editor which is built in the HyperChem software. In order to find global minimum the Molecular Dynamics [44] with MM+ forcefield [45] was used. Dynamics was performed at the simulation temperature 2000 K with run time 750 ps. The run time was divided to five frames from which there were 25 starting geometries selected. These different starting structures of conformer were refined by molecular mechanics and re-optimized by AM1 method. The RMS gradient 0.01 kcal/(A mol) as a convergence criterion was used for all calculations and the RMS Fit describing differences among geometries of conformers with the minimum energy had the order of 10^{-5}.

4. Results and discussion

From Eqs. (2) and (3), it follows that the determination of the energy barrier to enantiomerization using dynamic chromatography is based on the peak areas of enantiomers of individual enantiomers prior to (A_{A0}, A_{B0}) and after the separation (A_A, A_B).

The following assumptions are considered prior to determination of enantiomer peak areas by the computer-assisted peak deconvolution method of chromatograms obtained by separating a racemic mixture [23,32]:

(a) Enantiomer peak areas prior to separation of a racemic mixture can be determined from a peak

cluster envelope area registered on an experimental chromatogram:

$$A_{A0} = A_{B0} = (A_A + A_B + A_{A'B'})/2 \quad (6)$$

(b) Response of a chromatographic detector for enantiomers (A, B) and that arose during enantiomerization (A', B') is equal.

(c) Enantiomers that arose during enantiomerization (A', B') are eluted in: (i) a broad peak between the peaks of enantiomers supposing that the peak cluster consists of three peaks (in the three peak concept); (ii) two broad peaks between the peaks of enantiomers supposing that the peak cluster consists of four peaks (in the four peak concept).

(d) Peaks profiles of enantiomers (A, B) and products of enantiomerization (A', B') can be described by Gaussian or exponentially modified Gaussian functions.

In our previous papers [22,35,39] we reported that the peak cluster of enantiomers arose by dynamic chromatography consists of three peaks containing original A, B and interconverted A', B' enantiomers. Differences between the area of experimental and calculated peak clusters listed in Table 1, however, indicated that instead of three peaks four peaks should be used in the deconvolution. Four peaks concept was recently proposed also by Marriot et al. [46] procedure. Fig. 3 shows the peak cluster obtained for enantiomers of *N*-(*p*-methoxybenzyl)-1,3,2-benzodithiazol-1-oxide by SFC at 50 °C and the peaks obtained by a deconvolution procedure with three (Fig. 3A) and four (Fig. 3B) peak

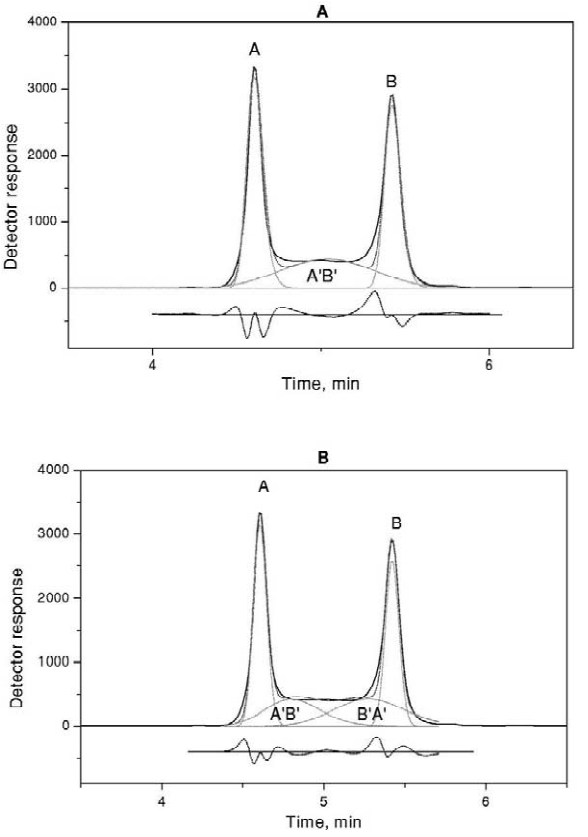

Fig. 3. Isocratic separation of enantiomers of *N*-(*p*-methoxybenzyl)-1,3,2-benzodithiazol-1-oxide by SFC at 50 °C with a mobile phase (2 ml min^{-1} of supercritical carbon dioxide containing 20% of methanol) at a pressure of 200 bar. (—) denotes peak envelope for experimental chromatogram, (· · ·) denotes computer-assisted deconvoluted peaks, (- – - –) denotes peak envelope for computer-reconstructed chromatogram.

Table 1
Apparent rate constant k_1^{app} and energy barrier to $A \rightarrow B$ enantiomerization ($\Delta G_{R\rightarrow S}^{app}$) determined for *N*-(*p*-methoxybenzyl)-1,3,2-benzodithiazol-1-oxide by DSFC for irreversible concept found by deconvolution of peak clusters using three- and four-peak concepts at various temperatures

Temperature (°C)	Three-peak concept			Four-peak concept		
	k_1^{app} Eq. (1a)	$\Delta G_{A\rightarrow B}^{app}$ (kJ mol^{-1})	%Δ	k_1^{app} Eq. (2a)	$\Delta G_{A\rightarrow B}^{app}$ (kJ mol^{-1})	%Δ[a]
35	1.7 E-4	96.0	1.4	2.26 E-4	93.7	0.9
40	4.57 E-4	95.0	3.3	5.24 E-4	94.7	0.01
45	1.12 E-3	94.2	0.03	9.12 E-4	93.3	0.19
50	1.02 E-3	96.0	0.3	1.55 E-3	94.9	0.96
55	2.03 E-3	95.6	3.4	2.53 E-3	95.0	2.3
60	3.47 E-3	95.7	4.0	2.95 E-3	96.0	0.47

[a] $\%\Delta = 100\ (\Sigma A_{exp} - \Sigma A_{dec})/\Sigma A_{exp}$, where ΣA_{exp} is an experimental and ΣA_{dec}—is a deconvoluted peak cluster area.

concepts. Peaks of original (A, B) and interconverted (A', B') enantiomers are drawn in Fig. 3 using dotted lines by a computer-assisted procedure built in Origin software. An exponentially modified Gauss peak shape fitting function was used to deconvolute the peak cluster in this work [40,41]. Since the original (A, B) and interconverted (A', B') enantiomers elute through the column independently, and the interconversion is characterised as an irreversible reaction [36], four peaks are expected in the peak cluster, as shown in Fig. 4 for the DSFC separation of lorazepam enantiomers. These four peaks arose from an independent interconversion of A and B enantiomers as shown in Fig. 4A,B. To distinguish between the species that arose from the first and second eluted enantiomers, respectively, they are labelled as $A'B'$ and $B'A'$, in Figs. 3 and 4. Our results show that the computer-assisted deconvolution of the peak cluster based on the concept of four peaks (Fig. 4D) leads to results analogous to those obtained by the DSFC of pure enantiomers [47].

Figs. 5–7 show the temperature dependence of the peak cluster shapes of lorazepam, temazepam and oxazepam enantiomers separated by DSFC throughout the whole range of $A \rightarrow B$ and $B \rightarrow A$ enantiomerization. The peak clusters on the experimental chromatograms shown in Figs. 5–7 were deconvoluted using Origin software and the four-peak concept as depicted in Fig. 4D. The peak areas A_{A0}, A_{B0}, A_A, and A_B determined with this procedure were used to calculate the apparent rate constants and apparent energy barriers to enantiomerization of all studied 3-hydroxy-1,4-benzodiazepine enantiomers. Tables 2–5 list the apparent rate constants (k_1^{app}) and energy barriers to enantiomerization (ΔG_1^{app}) determined for $A \rightarrow B$ enantiomerization of lorazepam, temazepam and oxazepam enantiomers by DSFC at various temperatures, using equations for the reversible (Eqs. (1a) and (3a)) and irreversible (Eqs. (2a) and (3a)) approaches. The data listed in Tables 2–4 for lower temperatures (30–40 °C for lorazepam, 30–50 °C for temazepam and 30–35 °C for oxazepam) determined both for reversible and irreversible concepts are in a reasonable agreement. It should, however, be noticed that data at 30 °C are not obtained fully at SFC conditions, since the critical temperature of CO_2 is 31 °C. This difference is responsible for separation process but does not influence the determination of enantiomerizationm energy barrier. Data at higher temperatures (>40 °C for lorazepam, >50 °C for temazepam and >35 °C for oxazepam) for reversible concept, however, could not be calculated by Eq. (1a). The greater range of conditions amenable to the irreversible concept approach is evident. The last column in Tables 2–4 shows differences between the experimental and deconvoluted peak cluster areas, which do not exceed 2.5% rel.

Tables 5–7 show the data obtained by isothermal DSFC separation of the enantiomers of lorazepam, temazepam and oxazepam enantiomers using different mobile phase flow-rates.

The flow dependence measurements were performed with the same mobile phase composition and pressure as listed in Fig. 4. Mean values calculated from Tables 5–7 for the apparent energy of $A \rightarrow B$ enantiomerization at 45 °C ($\Delta G_{A\rightarrow B}^{app} = 90.4$ for lorazepam, $\Delta G_{A\rightarrow B}^{app} = 94.1$ for temazepam and $\Delta G_{A\rightarrow B}^{app} = 89.8$ for oxazepam) are shown for enantiomers of the corresponding 3-hydroxy-1,4-benzodiazepines listed in Tables 5–7.

Fig. 8 shows the dependence of enantiomerization energy barrier ($\Delta G_{A\rightarrow B}^{app}$) on temperature (K) found by SFC for the first eluted enantiomers of lorazepam (A), temazepam (B) and oxazepam (C). For the construction of plots in Fig. 8, data listed in Tables 2–4 were used. Using Eq. (6), the activation enthalpy ($\Delta H_{A\rightarrow B}^{app}$) and entropy ($\Delta S_{A\rightarrow B}^{app}$) were calculated from dependencies shown in Fig. 8 as slopes and intercepts, respectively. The obtained results as well as rate constants and half-lives ($t_{1/2}$) at 303 K are listed in Table 8. Mean values calculated from the dependences shown in Fig. 8 for the apparent energy of $A \rightarrow B$ enantiomerization at 45 °C ($\Delta G_{A\rightarrow B}^{app} = 91.8$ for lorazepam, $\Delta G_{A\rightarrow B}^{app} = 94.4$ for temazepam and $\Delta G_{A\rightarrow B}^{app} = 91.7$ for oxazepam) are overlapped within ±2% from the data listed above as the mean values calculated for enantiomers of the corresponding 3-hydroxy-1,4-benzodiazepines from data listed in Tables 5–7. Comparison of data obtained in this study with those published by Schurig with co-workers [19] shows very good consistency of enantiomerization energy barrier for lorazepam and temazepam (differences lower than 1%rel) and acceptable consistency for temazepam (difference around 2.6% rel.). The different tempera-

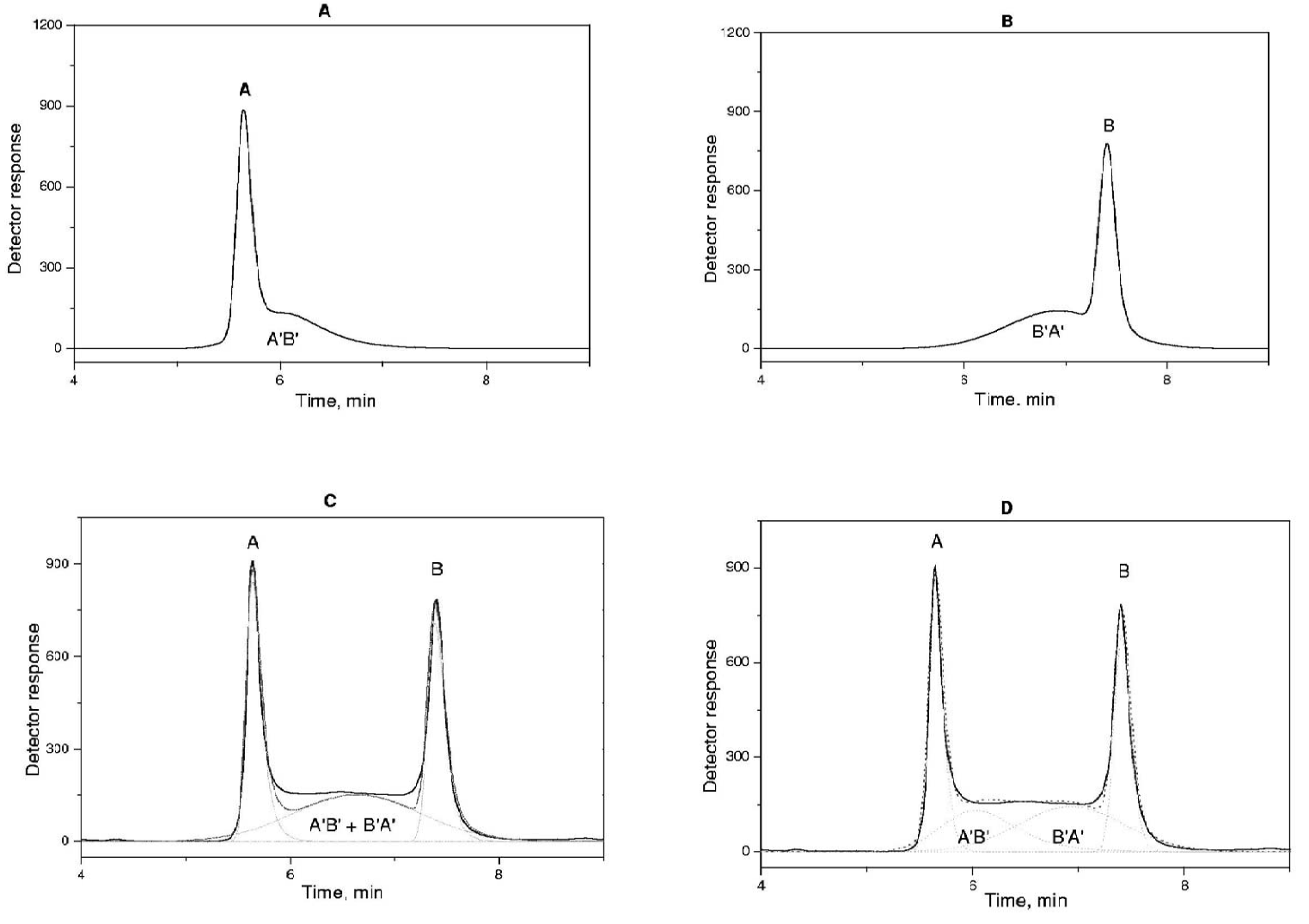

Fig. 4. Isocratic separation of enantiomers of lorazepam by SFC at 40 °C with a mobile phase (2 ml min^{-1} of supercritical carbon dioxide containing 12.5% methanol with 0.5% diethylamine as modifier) at a pressure of 200 bar. (—) Peak envelope for experimental chromatogram; (· · ·) computer-assisted deconvoluted peaks; (- – - –) peak envelope for computer-reconstructed chromatogram.

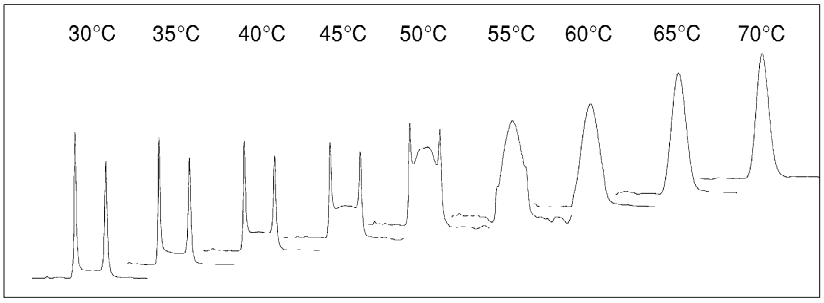

Fig. 5. Temperature dependence of peak clusters obtained by the separation of enantiomers of lorazepam by SFC. Isocratic flow of mobile phase (2 ml min^{-1} of supercritical carbon dioxide containing 12.5% methanol with 0.5% diethylamine as modifier) at a pressure of 200 bar. For other details see Section 3.

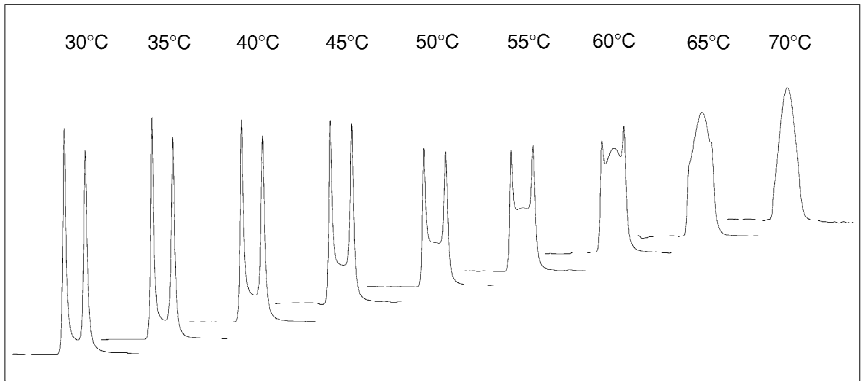

Fig. 6. The separation of temazepam enantiomers by SFC at 60 °C, at various inlet pressures of mobile phase. Isocratic flow of mobile phase (2 ml min^{-1} of supercritical carbon dioxide containing 12.5% methanol with 0.5% diethylamine as modifier) at a pressure of 200 bar. For other details see Section 3.

tures at which the data are compared in Table 8 and the correlation coefficients found for plots in the Fig. 8 ($r=0.916$ for lorazepam, $r=0.988$ for temazepam and $r=0.994$ for oxazepam), which were lower than that published by Schurig with co-workers [19], can explain differences in other kinetic activation data.

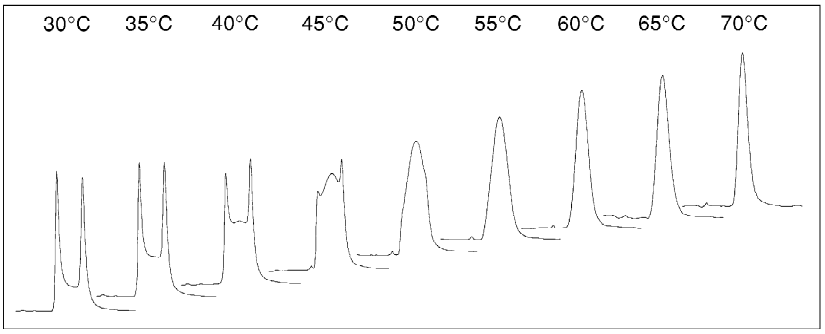

Fig. 7. The separation of oxazepam enantiomers by SFC at 60 °C, at various inlet pressures of mobile phase. Isocratic flow of mobile phase (2 ml min^{-1} of supercritical carbon dioxide containing 12.5% methanol with 0.5% diethylamine as modifier) at a pressure of 200 bar. For other details see Section 3.

Table 2
Apparent rate constant k_1^{app} and energy barrier to $A \rightarrow B$ enantiomerization ($\Delta G_{A\rightarrow B}^{app}$) determined for lorazepam by DSFC at various temperatures

Temp. (°C)	Reversible concept		Irreversible concept		%Δ[a]
	k_1^{app} (s^{-1}) Eq. (1a)	$\Delta G_{A\rightarrow B}^{app}$ (kJ mol^{-1})	k_1^{app} (s^{-1}) Eq. (2a)	$\Delta G_{A\rightarrow B}^{app}$ (kJ mol^{-1})	
30	7.77 E-4	90.6	6.79 E-4	90.9	0.54
35	2.05 E-3	89.6	1.40 E-3	90.6	0.62
40	5.77 E-3	88.4	1.83 E-3	91.5	2.13
45	–	–	2.74 E-3	91.9	0.01
50	–	–	4.37 E-3	92.1	1.92

[a] See footnote in Table 1.

Table 3
Apparent rate constant k_1^{app} and energy barrier to $A \rightarrow B$ enantiomerization ($\Delta G_{A\rightarrow B}^{app}$) determined for temazepam by DSFC at various temperatures

Temp. (°C)	Reversible concept		Irreversible concept		%Δ[a]
	k_1^{app} (s^{-1}) Eq. (2a)	$\Delta G_{A\rightarrow B}^{app}$ (kJ mol^{-1})	k_1^{app} (s^{-1}) Eq. (5)	$\Delta G_{A\rightarrow B}^{app}$ (kJ mol^{-1})	
30	2.03 E-4	93.9	1.95 E-4	94.0	0.50
35	4.77 E-4	93.3	4.33 E-4	93.6	1.15
40	7.93 E-4	93.6	6.73 E-4	94.0	1.11
45	1.52 E-3	93.4	1.09 E-3	94.3	1.76
50	3.05 E-3	93.1	1.52 E-3	94.9	0.68
55	–	–	2.43 E-3	95.2	0.36
60	–	–	3.25 E-3	95.8	0.47

[a] See footnote in Table 1.

The highest interconversion barrier ($\Delta G_{A\rightarrow B}^{app}$) and consequently the highest half-live ($t_{1/2}$) were found for temazepam. This could be caused by an induction effect of the methyl group, which limits the interconversion. Comparison of data listed in Table 8 shows that the lowest enantiomerization barrier belongs to oxazepam. The 2′ chlorine constituent in lorazepam slightly stabilizes this system which results in an increase of its interconversion barrier and half-live. Entropic terms, however, show a more complicated correlation with the molecular mass. This indicates that apparent entropy is influenced

Table 4
Apparent rate constant k_1^{app} and energy barrier to $A \rightarrow B$ enantiomerization ($\Delta G_{A\rightarrow B}^{app}$) determined for oxazepam by DSFC at various temperatures

Temp. (°C)	Reversible concept		Irreversible concept		%Δ[a]
	k_1^{app} (s^{-1}) Eq. (2a)	$\Delta G_{A\rightarrow B}^{app}$ (kJ mol^{-1})	k_1^{app} (s^{-1}) Eq. (5)	$\Delta G_{A\rightarrow B}^{app}$ (kJ mol^{-1})	
30	1.04 E-3	89.8	9.75 E-4	90.0	0.49
35	1.62 E-3	90.2	1.14 E-3	91.1	1.10
40	–	–	2.15 E-3	91.0	2.26

[a] See footnote in Table 1.

Table 5
Apparent rate constant k_1^{app} and energy barrier to $A \rightarrow B$ enantiomerization ($\Delta G_{A\rightarrow B}^{app}$) determined for lorazepam by DSFC with various mobile phase flow at 45 °C

Flow (ml min^{-1})	Reversible concept		Irreversible concept		
	k_1^{app} (s^{-1}) Eq. (1a)	$\Delta G_{A\rightarrow B}^{app}$ (kJ mol^{-1})	k_1^{app} (s^{-1}) Eq. (2a)	$\Delta G_{A\rightarrow B}^{app}$ (kJ mol^{-1})	%Δ[a]
1.2	–	–	3.48 E-3	89.8	0.63
1.6	–	–	2.87 E-3	90.3	0.21
2.0	–	–	2.65 E-3	90.5	0.68
2.4	–	–	2.08 E-3	91.1	1.46

[a] See footnote in Table 1.

Table 6
Apparent rate constant k_1^{app} and energy barrier to $A \rightarrow B$ enantiomerization ($\Delta G_{A\rightarrow B}^{app}$) determined for temazepam by DSFC with various mobile phase flow at 45 °C

Flow (ml min^{-1})	Reversible concept		Irreversible concept		%Δ[a]
	k_1^{app} (s^{-1}) Eq. (2a)	$\Delta G_{A\rightarrow B}^{app}$ (kJ mol^{-1})	k_1^{app} (s^{-1}) Eq. (5)	$\Delta G_{A\rightarrow B}^{app}$ (kJ mol^{-1})	
1.6	8.56 E-4	93.5	6.74 E-4	94.1	0.04
2.4	7.30 E-4	93.8	6.46 E-4	94.2	1.94

[a] See footnote in Table 1.

Table 7
Apparent rate constant k_1^{app} and energy barrier to $A \rightarrow B$ enantiomerization ($\Delta G_{A\rightarrow B}^{app}$) determined for oxazepam by DSFC with various mobile phase flow at 45 °C

Flow (ml min^{-1})	Reversible concept		Irreversible concept		%Δ[a]
	k_1^{app} (s^{-1}) Eq. (2a)	$\Delta G_{A\rightarrow B}^{app}$ (kJ mol^{-1})	k_1^{app} (s^{-1}) Eq. (5)	$\Delta G_{A\rightarrow B}^{app}$ (kJ mol^{-1})	
2.0	–	–	3.45 E-3	89.8	1.26
2.4	–	–	3.49 E-3	89.8	2.81

[a] See footnote in Table 1.

Table 8
Kinetic activation parameters of the enantiomerization of lorazepam, temazepam and oxazepam obtained by SFC at 313 K and published at 293 K [19]

Compound	$\Delta G_{A\rightarrow B}^{app}$ (kJ mol^{-1})	$\Delta H_{A\rightarrow B}^{app}$ (kJ mol^{-1})	$\Delta S_{A\rightarrow B}^{app}$ (J (K mol)$^{-1}$)	k_1^{app} (s^{-1})	$t_{1/2}$ (min)
Lorazepam	91.8	68.2	−40.6	1.83 E-3	6.3
	91.4[a]	76.5[a]	−50.9[a]	3.1 E-4[a]	34.9[a]
Temazepam	94.0	66.8	−86.9	6.73 E-4	17.2
	91.6[a]	90.5[a]	−3.9[a]	2.9 E-4[a]	39.8[a]
Oxazepam	91.0	59.9	−100	2.15 E-3	5.4
	91.4[a]	72.0[a]	−65.8[a]	3.3 E-4[a]	37.3[a]

[a] Data published by Schurig with co-workers [19].

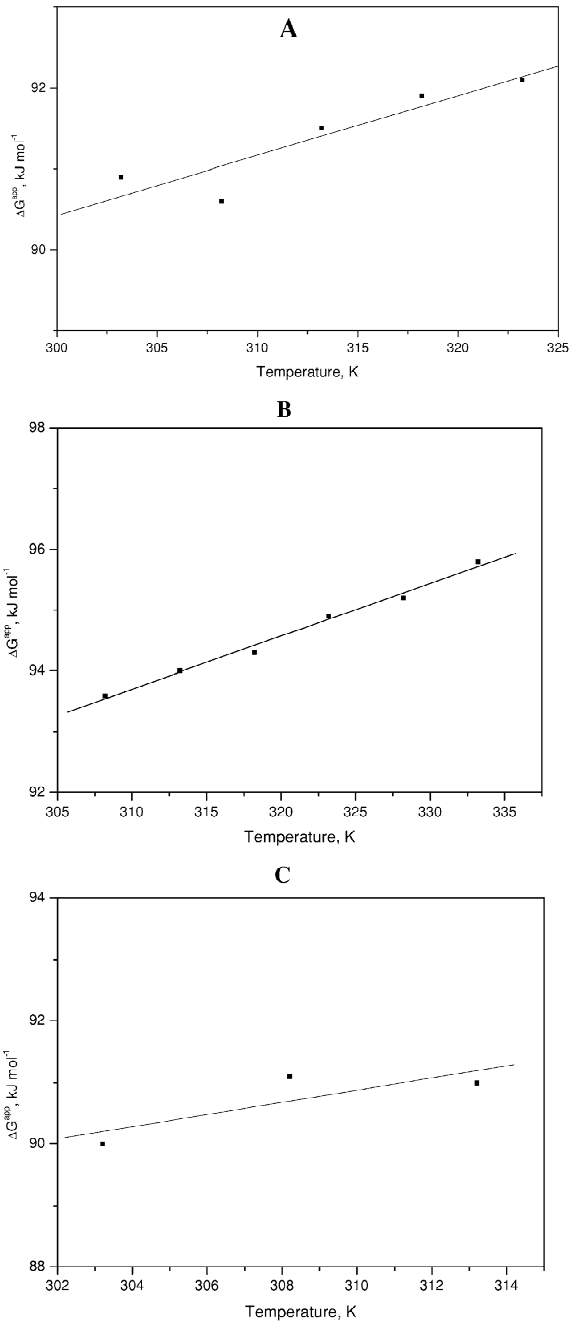

Fig. 8. Dependence of free energy of enantiomerization ($\Delta G^{app}_{A\rightarrow B}$) on temperature (T) for lorazepam (A), temazepam (B) and oxazepam (C).

inter alia both with molecular mass as well by structural factors and interactions occurring during the separation procedure.

Acknowledgements

PO, JK and PM acknowledge the support of the Grant Agency of Slovak Slovak Republic (VEGA 1/9127/02) and the Agency for International Science and Technology Cooperation in Slovakia (Grant No. 002-98). DWA acknowledges the support of the National Institutes of Health (Grant NIH R01 GM 53825-05).

References

[1] FDA, Chirality 4 (1992) 338.
[2] S. Garatini, E. Mussini, L.O. Randal (Eds.), The Benzodiazepines, Raven Press, New York, 1973.
[3] H. Möhler, T. Okada, Science 198 (1977) 849.
[4] W.E. Müller, U. Wollert, Mol. Pharmacol. 11 (1975) 52.
[5] M. Rizzo, Rev. J. Chromatogr. B 747 (2000) 203.
[6] C. Villani, W.H. Pirkle, Tetrahedron: Asymmetry 6 (1995) 27.
[7] A. Fell, T.A.B. Noctor, J.E. Mama, B.J. Clark, J. Chromatogr. 434 (1988) 377.
[8] X.-L. Lu, S.K. Yang, J. Chromatogr. A 535 (1990) 229.
[9] T. Jira, C. Vogt, G. Blaschke, T. Beyrich, Pharmazie 48 (1993) 196.
[10] E. Chosson, S. Uzan, F. Gimenez, I.W. Wainer, R. Farinotti, Chirality 5 (1993) 71.
[11] I. Fitos, J. Visy, M. Simonyi, J. Hermansson, J. Chromatogr. A 709 (1995) 265.
[12] V. Andrisano, T.D. Booth, V. Cavrini, I.W. Wainer, Chirality 9 (1997) 178.
[13] T. Nishikawa, Y. Hayashi, S. Suzuki, H. Kubo, H. Ohtani, J. Chromatogr. A 767 (1997) 93.
[14] A.M. Stalcup, W. Wu, K.L. Williams, Biomed. Chromatogr. 11 (1997) 325.
[15] K. Krause, M. Girod, B. Chankvetadze, G. Blaschke, J. Chromatogr. A 837 (1999) 51.
[16] H. Kanazawa, Y. Kunito, Y. Matsushima, S.H. Kanazawa, Y. Kunito, Y. Matsushima, S. Okubo, F. Mashige, J. Chromatogr. A 871 (2000) 181.
[17] C. Wolf, W.H. Pirkle, C.J. Welch, D.H. Hochmuth, W.A. König, G.-L. Chee, J.L. Charlton, J. Org. Chem. 62 (1997) 5208.
[18] J.L. Haynes III, E.J. Billiot, H.H. Yarabe, I.M. Warner, S.A. Shamsi, Electrophoresis 21 (2000) 1597.
[19] G. Schoetz, O. Trapp, V. Schurig, Anal. Chem. 72 (2000) 2758.
[20] S. Wang, M.D. Porter, J. Chromatogr. A 828 (1998) 157.
[21] K. Krause, M. Girod, B. Chankvetadze, G. Blaschke, J. Chromatogr. A 837 (1999) 51.
[22] P. Oswald, J. Krupcík, I. Spánik, M. Bajdichová, P. Sandra, D.W. Armstrong, in: Proceedings of the First International Symposium on Advances in Chromatographic and Electrophoretic Separations University Bayreuth, Germany, April 16–18, 2000, 2000.

[23] W. Bürkle, H. Karfunkel, V. Schurig, J. Chromatogr. 288 (1984) 1.
[24] M. Jung, V. Schurig, J. Am. Chem. Soc. 114 (1992) 529.
[25] A. Mannschreck, H. Zinner, N. Pustet, Chimia 43 (1989) 165.
[26] J. Veciana, M.I. Crespo, Angew. Chem., Int. Ed. Engl. 30 (1991) 74.
[27] G. Weseloh, C. Wolf, W.A. König, Angew. Chem. 107 (1995) 1771.
[28] V. Schurig, A. Glausch, M. Fluck, Tetrahedron: Asymmetry 6 (1995) 2161.
[29] G. Weseloh, C. Wolf, W.A. König, Chirality 8 (1996) 441.
[30] S. Reich, V. Schurig, in: P. Sandra, A.J. Rackstraw (Eds.), Proceeding of the 20th International Symposium on Capillary Chromatography, 1998 I.O.P.M.S. vzw., Kortijk Belgium, J.13, 1998.
[31] V. Schurig, S. Reich, Chirality 10 (1998) 425.
[32] O. Trapp, G. Schoetz, V. Schurig, Chirality 13 (2001) 403.
[33] M. Štromar, V. Šunjič, T. Kovač, L. Klasinic, F. Kajfež, Croatica Chem. Acta 46 (1974) 265.
[34] A. Kot, P. Sandra, A. Venema, J. Chromatogr. Sci. 32 (1994) 439.
[35] P. Oswald, K. Desmet, P. Sandra, J. Krupcik, D.W. Armstrong, Analusis 28 (2000) 859.
[36] J. Krupcik, P. Oswald, K. Desmet, P. Sandra, D.W. Armstrong, Chirality 14 (2002) 334.
[37] P.W. Atkins, in: Physical Chemistry, 5th Edition, Oxford University Press, Oxford, 1995.
[38] J. Hrouzek, J. Krupcik, M. Ceppan, S. Hatrik, P.A. Leclercq, Chem. Papers 54 (2000) 315.
[39] J. Krupcík, P. Oswald, I. Spánik, P. Májek, M. Bajdichová, P. Sandra, D.W. Armstrong, J. Microcol. Sep. 12 (2000) 630.
[40] Microcal™ Origin™ Version 4.10, Microcal Software, One Roundhouse Plaza, Northampton, MA, 01060 USA.
[41] Peak Fitting Module, Microcal Software, Inc., Northampton, MA, USA
[42] M.J.S. Dewar, E.G. Zoebisch, E.F. Healy, J.J.P. Stewart, AM1: A new general purpose quantum mechanical model, J. Am. Chem. Soc. 107 (1985) 3902.
[43] HyperChem Release 3 for Windows, Hypercube, 1993.
[44] W.F. van Gunsteren, H.J.C. Berendsen, Ang. Chem., Int. Ed. Eng. 29 (1990) 992.
[45] N.L. Allinger, J. Am. Chem. Soc. 99 (1977) 8127.
[46] P. Marriott, O. Trapp, R. Shellie, V. Schurig, J. Chromatogr. A 919 (2001) 115.
[47] P. Oswald, K. Desmet, P. Sandra, J. Krupcik, D.W. Armstrong, Presented at 25th International Symposium on Capillary Chromatography, Palazzo dei Congressi, Riva del Garda, Italy, May 13–17 2002, G.04.